Journal of Non-Crystalline Solids 594 (2022) 121821

Contents lists available at ScienceDirect

Journal of Non-Crystalline Solids

journal homepage: www.elsevier.com/locate/jnoncrysol

Hierarchical macro to nano press molding of optical glasses by using metallic glasses

Fei Sun [1], Jian Yang [1], Jianan Fu, Bei Wang, Jiang Ma [*], Jun Shen

Shenzhen Key Laboratory of High Performance Nontraditional Manufacturing, College of Mechatronics and Control Engineering, Shenzhen University, Shenzhen 518060, China

ARTICLE INFO

Keywords:
Precision glass molding
Metallic glass
Hierarchical metal mold
Nano-lens arrays

ABSTRACT

The fabrication of ideal optical components is a world-wide grand challenge facing us. Benefiting from the unique thermoplastic nature, precision glass molding (PGM) is considered as a promising method for rapid and precise fabrication of optical components. The success and proliferation of such methods critically rely on the manufacturing of robust and durable master molds. Although silicon-based molds relying on photolithographic forming are facile to manufacture, they are brittle and have limited longevity when used as the molds. To address this challenge, here, we propose a hierarchical macro to nano mold preparation method based on the thermoplastic forming ability of metallic glasses (MGs), which excels in micro and nano scale fabrication. After subsequently crystallizing the as-formed MG, we demonstrate that the crystalline MG is suitable as an excellent mold for molding optical glasses with service temperature up to 600 °C. Using this 'spawning' process, several metallic molds including macroscopic lens arrays, microscale gratings, and nano-lens arrays were successfully prepared, respectively. The minimum feature size of the mold is 300 nm and the optimum surface roughness is 7.43 nm. Correspondingly, we prepared hierarchical optical glass components with excellent optical properties using MG as molds.

1. Introduction

In recent optical and biomedical industries, great demands of optical components are in need, especially those with micro structure surface that could yield new light functions [1–3]. Glasses and plastics are commonly used substrate materials to fabricate such products. Owing to the significant advantages on aspects of hardness, refractive index, light permeability and environmental stability, glasses usually play irreplaceable roles in the fields of aerospace and national defense which requires high quality [4–7]. However, precision forming is still a huge challenge for glass due to its high hardness and brittleness. Conventional grinding and polishing are mature methods to prepare optical elements of macro scale, on the down side, they are expensive, time consuming and not capable for the micro/nano structure surface fabrication of glasses [8–11]. Although sand blasting, photolithography, wet/dry etching and micro cutting techniques have been developed to construct micro/nano patterns on glasses, they are either of poor accuracy, low efficiency or high cost, hence not appropriate for the massive production of glass components [12–15]. Therefore, many researchers are interested in the development of a new glass processing method.

Benefiting from the thermoplastic forming ability, precision glass molding (PGM) is considered as a very promising approach to achieve fast and precise fabrication of optical components. It has raised enormous attention since proposed to produce precision optical elements such as aspherical lenses, Fresnel lenses, diffractive optical elements (DOEs), micro lens arrays and so on [16–21]. In the glass thermo molding process, mold materials and mold fabrication stands as a longstanding important issue to be satisfactorily solved. The mold materials are required to have superior high temperature strength as well as harness, workability, stability, dimensional accuracy and low cost *et al.* Generally speaking, hard materials such as silicon carbide (SiC), tungsten carbide (WC) and fused silica (SiO_2) are preferable mold materials. Unfortunately, they are merely suitable for the macro scale continuous mold surfaces, the case would be very difficult if one wants to generate micro/nano structures on these materials [22]. Previous research preliminary has demonstrated that the micro cutting of surface plating (e. g. Ni-P or Ni-W coating) on stainless steel can be used for the glass components molding with micro structures, however, the whole process is

* Corresponding author.
E-mail address: majiang@szu.edu.cn (J. Ma).
[1] These authors contributed equally to this work.

https://doi.org/10.1016/j.jnoncrysol.2022.121821
Received 6 June 2022; Received in revised form 15 July 2022; Accepted 16 July 2022
Available online 22 July 2022
0022-3093/

complex and not environmental friendly, more importantly, the endurable temperature of the mold is limited [21]. Apart from this, with the rising requirements of optical components with higher quality, the fabrication of small structures down to nano scale is the inevitable tendency, and it should be noted that the glass molding on length scale from several micro to nanometers is still a big challenge. Silicon (Si) is another mold option for the micro even nano forming of glasses, unfortunately, due to the high susceptibility to wear and tear and severe adhesion to glass in high temperature, Si mold is not suitable for PGM. Hence, it is significant to find novel mold materials and techniques for glass molding of micro and nano scale components.

Metallic glasses (MGs) are a class of metallic materials without long-range ordering crystalline structures. The unique amorphous nature endows them with ultrahigh strength and hardness, high wear and corrosion resistances [23–25]. Interestingly, MGs can be thermoplastically formed like plastics in a temperature window known as the supercooled liquid region (SLR) [26]. Benefitting from this window, MGs can be easily formed into complex surface structures with well-defined geometries on length scales ranging from macro-, micro- and nano-scale [27–30]. The unique characteristics of MG can provide an economical and convenient avenue for precision manufacturing of embossing molds [31,32]. Unfortunately, the relatively low glass transition temperature (T_g, generally lower than 400 °C) of MGs limits their applicability to the molding of plastic polymers with similarly lower T_g (generally lower than 200 °C) [33–36], while applications to the molding of optical glasses with high T_g (>500 °C) have merely been reported. In this work, based on the thermoplastic properties of MGs, we developed a "crystallization after forming" strategy to achieve precision fabrication of hierarchical glass molding molds from the macro to nano scale. The obtained molds can endure high temperatures up to 600 °C, which is suitable for the molding of most optical glasses. Our results provide a fast and cost-efficient method for the mass production of optical molds and throw light on the precision fabrication of nanoscale glass optical devices.

2. Experimental

2.1. Materials & mold preparation

The $Zr_{55}Cu_{30}Ni_5Al_{10}$ (at.%) MG was chosen for this study owing to its excellent glass forming ability and thermoforming ability [37], which ensure the retention of amorphous nature during the structure construction process. The alloy ingots were prepared by arc melting a mixture of elements with a purity at least 99.95% under a Ti-gettered purified Ar atmosphere. To ensure a homogeneous composition, each ingot was remelted five times. Afterwards, MG rods with a diameter of 5 mm were obtained by casting the melted alloy into a copper mold. The tungsten carbide balls (WC-8 wt.% Co) with diameters of 5 mm and 1 mm, grating patterned Si templates with line width and depth of 10 μm and anodic aluminum oxide (AAO) plate with a pore size of ~300 nm was purchased directly from commercial suppliers and act as precursor molds to thermoform macro, micro and nano scale structure on the surface of MGs, respectively. After that, the structured MG was fully crystallized under high temperature above crystallization temperature (T_x) for 30 min. Then, crystallized MG (CMG) was used as mold to thermoform optical glasses. The optical glass, D-K59 (Ø5 mm, 2 mm thick, CDGM Glass Co. Ltd., China) was chosen for this work, and the T_g is 497 °C and softening temperature (T_s) is 551 °C, respectively. Both MG and glass billets were polished to an optical mirror surface with a roughness of less than 5 nm prior to thermoforming.

2.2. Characterizations

The intrinsic structure of the as-cast, thermoformed and crystallized MGs were ascertained by x-ray diffraction (XRD; Rigaku MiniFlex600) with Cu Kα radiation and differential scanning calorimetry (DSC; Perkin–Elmer DSC-8000) at a heating rate of 20 °C/min. The high-temperature contact angle (HCA) between mold materials and molten glass was determined by a droplet shape analyzer (DSA100S, Krüss, Germany). The microscopic morphology of the precursor molds, MG molds and the final obtained optical components were collected by a scanning electron microscope (SEM; FEI QUANTA FEG 450) instrument. The three-dimensional (3D) morphology and dimensional accuracy of microscale molds as well as optical components were evaluated utilizing white-light interfering profilometer (Bruker ContourGT-X 3D). The 3D profiles of nanoscale molds and corresponding optical components were measured using atomic force microscopy (AFM, OXFORD MFP-3DInfinity). The transmittances of the bare and nanoimprinted glass were measured and evaluated by adopting a commercial Fourier transform spectrometer (Shimadzu UVmini-1280, Japan).

2.3. Experimental setup

The thermoplastic forming of CMG molds and optical glass components was carried out on self-developed equipment (TM-YJ-03, ShenZhen University, China). The equipment uses resistance heating, with a maximum temperature of 1200 °C and an accuracy of ±2 °C. The pressure system is based on a closed-loop servo-cylinder output and is available in the load range 0.2–30 kN, with an accuracy of 0.01 kN. The ultimate vacuum of the equipment is 3 × 10–4 pa, the cooling method is circulating water cooling, the control system is developed on the basis of LabVIEW. The basic principle of the hierarchical press molding of optical glasses using MG molds was schematically drawn in Fig. 1(a). First, the precursor molds (WC balls, Si and AAO) and MG were sequentially assembled in the vacuum cavity and then a pre-pressure of 0.05 kN was applied. Subsequently, the cavity vacuum was pumped to 3×10^{-4} Pa to avoid oxidation of the molds and MG during the thermoplastic forming process. Then the chamber was heated up to 450 °C at a heating rate of 50 °C/min. The structure would transfer from the precursor templates to the MG with the application of certain force. The chamber was then continued to be heated to 550 °C and held for 30 min to ensure conversion of MG to CMG. After that, the CMG was used as the mold for the press molding of optical glasses.

3. Result and discussions

3.1. Surface quality evaluation of thermoformed mg and cmg

Fig. 1(b) presents the DSC curve of the as-cast MG, the typical glass transition phenomenon and exothermic crystallization peak can be found in this curve, indicating that the T_g is about 420 °C and T_x is about 480 °C, respectively. The XRD patterns in Fig. 1(c) compare the nature of MG and CMG. The typical crystal peaks can be found in the XRD pattern of CMG, while the amorphous peak can be found in the MG sample, reveals that the as-cast MG was fully amorphous nature and CMG was completely crystallized. In addition, the characteristic temperature point of CMG was also determined. Fig. 1(d) verifies the absence of amorphous phase in CMG and shows that the melting temperature (T_m) of CMG is 720 °C, reveals that the prepared CMG molds can form glasses with softening temperature higher than 600 °C.

The surface quality is a key concern for mold especially the optical component mold. To evaluate the effect of crystallization treatment on the surface roughness of MG, the polished Si wafers with a surface roughness of less than 5 nm were used as a precursor mold to thermoform MG at a load of 1 kN. Then the white light interferometer was used to characterize the surface quality of the thermoformed MG and corresponding CMG. As shown in Fig. 1(e-f), the overall surface roughness of MG obtained by hot pressing was 5.95 nm and the local roughness was 4.80 nm. The profiles in X and Y directions (see Fig. 1(g)) further demonstrate the value. Subsequently, the surface quality of the same area of the CMG corresponding to the MG was also evaluated. As presented in Fig. 1(h-j), the overall surface roughness of the CMG after

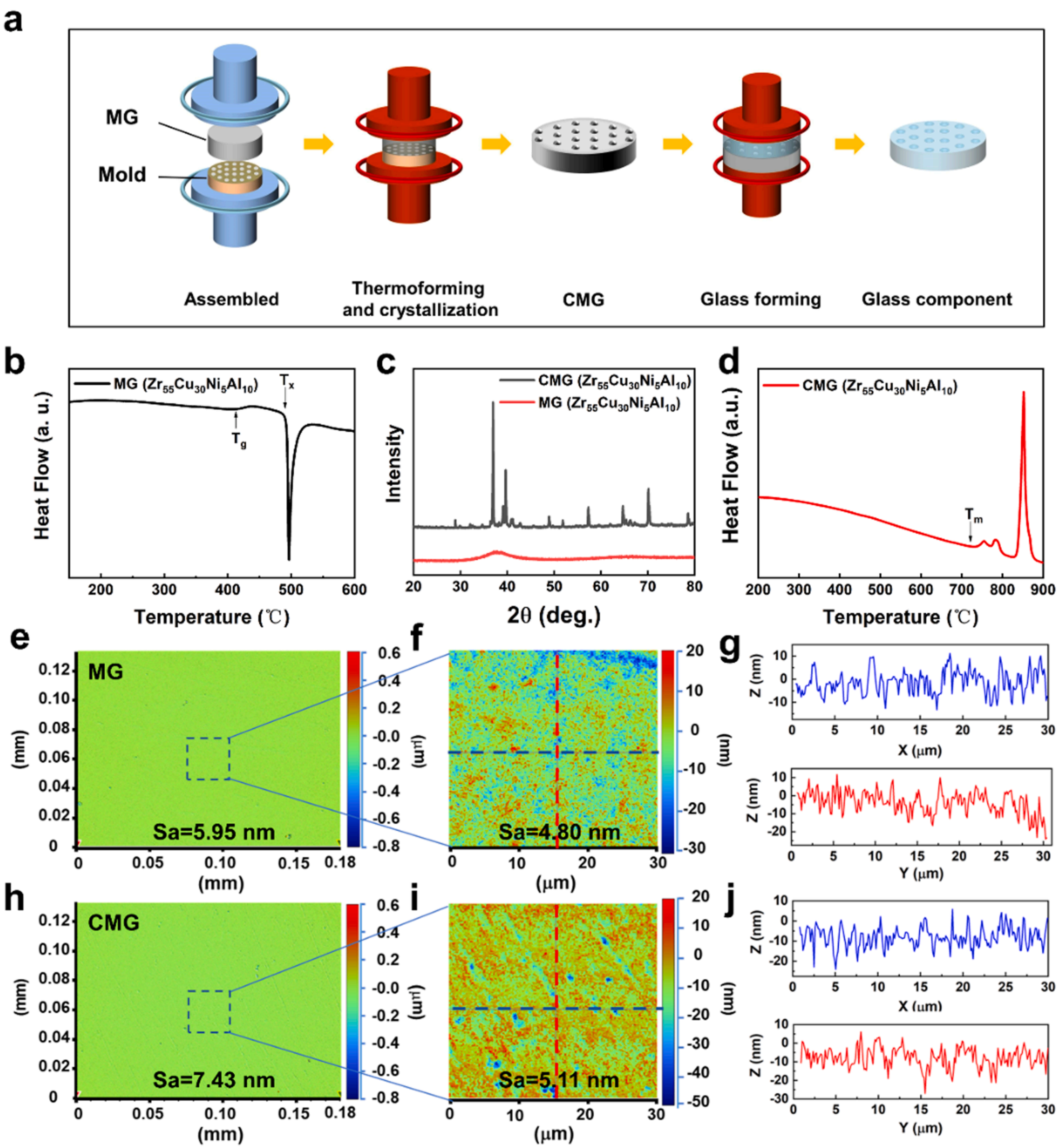

Fig. 1. (a) Schematic diagram of hierarchical optical component fabrication. (b) DSC curve of $Zr_{55}Cu_{30}Ni_5Al_{10}$. (c) XRD patterns of fully amorphous (MG) and crystallized (CMG) $Zr_{55}Cu_{30}Ni_5Al_{10}$. (d) DSC curve of CMG $Zr_{55}Cu_{30}Ni_5Al_{10}$. (e-g) Surface roughness of the MG obtained by hot pressing. (h-j) Surface roughness of CMG.

complete crystallization was 7.43 nm and the local roughness was 5.11 nm. It can be found that the surface roughness of CMG was merely increased by 1~2 nm compared to MG when avoiding oxidation, which is acceptable for the fabrication of optical molds.

3.2. Evaluation of adhesion of cmg mold to glasses

The phenomenon of glass-to-mold sticking is a major problem for PGM. Glass forming molds and forming tools work in a high temperature environment above 500 °C. The surface of the mold is highly vulnerable to reaction and adhesion with chemically active softened glass, which seriously depletes the life of the mold and damages the glass forming quality [38]. Therefore, it is essential to evaluate the anti-adhesion of CMG molds to glass at high temperatures. Measuring the high-temperature contact angle (HCA) between the molten glass and the mold is considered to be an intuitive and effective method [39–44]. In the present work, the glasses and the mold materials to be evaluated were heated to 700 °C in a vacuum environment and the contact between them is subsequently observed. Two other commonly used mold materials (WC and Si wafer) were also selected for the high-temperature wetting experiment for comparison. All mold materials were polished to an optical mirror finish prior to HCA experiments. The contact state of the mold materials with the molten glass was recorded and shown in Fig. 2(a-c), it can be found that CMG and WC exhibit a superior contact state with the molten glass, while Si shows severe adhesion to the molten glass. For a detailed comparison, the high-temperature contact angle (HCA) between the mold materials and molten glass was measured. According to Fig. 2(d-f), the HCA of CMG, WC and Si with molten glass were about 153.8°, 145.3° and 122.7°, respectively. This means that CMG exhibits even better glass adhesion resistance than the classic mold material WC. It is worth mentioning that the glass can detach freely from the CMG and WC after solidification, but adheres tightly to the Si wafer, which is consistent with the results of high temperature wetting experiments.

3.3. Preparation of multi-scale cmg molds and glass components

Tungsten carbide molds are widely used in PGM for macro glass parts due to their outstanding serviceability and excellent anti-adhesive properties with glasses [22]. However, with the dramatic increase in demand for lightweight and miniaturization of optical parts, the application of WC molds in glass molding is limited due to the extremely high manufacturing cost of micro and nano features. Leveraging the thermoplastic nature of MGs, CMG molds can obviate the challenges of micro and nano mold manufacturing. To verify the applicability, multi-scale CMG molds from macro to nano scale were prepared by thermoplastic forming. As shown in Fig. 3(a), a concave lens CMG mold with an aperture of 3 mm was easily prepared using a 5 mm diameter WC ball, one can find that the CMG mold possess obvious metallic luster. Fig. 3(b) shows the details of its appearance, no obvious defects and cracks can be observed. Furthermore, macroscopic lens array molds can also be fabricated using a similar method. As presented in Fig. 3(c), a macroscopic concave lens array CMG mold was prepared using multiple WC balls of 1 mm diameter. To validate the feasibility of the prepared CMG molds, optical glass (D-K59, T_g=497 °C, T_s=551 °C) was selected for the PGM experiment. The corresponding single lens and lenses arrays glass components were successfully prepared (see Fig. 3(d and f)). Fig. 3 (e) shows the lateral morphology of the glass lens in Fig. 3(d), and it can be found that the lens is clearly spherical, which is consistent with the characteristics of the WC ball.

Tungsten carbide and silicon carbide are considered to be excellent mold materials, but the manufacturing challenges severely limit their application in the field of micro and nano PGM. We demonstrate that CMG can be an excellent alternative material to solve the dilemma. To validate this, a Si template with a grating pattern was chosen to prepare the CMG mold. Fig. 3(g-i) present the morphology and dimensions of the original Si template. The pitch and depth of the gratings are both 10 µm. MG was converted into CMG after completing forming under a load of 0.5 kN. It can be found that the obtained CMG mold exactly replicates the structure of the Si template (see Fig. 3(j)). By comparing Fig. 3(h) and (k), we can find that the groove depth of the Si template is 8.82 µm, while the groove depth of the replicated CMG mold is 8.81 µm, it means that the replication accuracy of CMG can be as high as 99%. The comparison of the profile contours in Fig. 3(l) and (i) further demonstrates the precision replication capability of CMG. It is clear that the CMG mold is highly compatible with the structure of the Si template, which means that precision structures on CMG molds can be obtained by simple thermoforming instead of expensive special processing methods. Excitingly, utilizing the obtained CMG molds, similar structures were successfully prepared on optical glass. As shown in Fig. 3(m), a uniform and smooth grating structure was constructed on the glass surface. One can find that the line width of the raster on the glass is consistent with the CMG mold, which indicates the high applicability of the CMG mold in PGM. It is worth noting that the grating profile on the glass was curved rather than rectangular (see Figs. (m-o)), which was obtained by applying a tailored load. It means that glass grating components with different radii of curvature can be prepared to match different application scenarios, only by adjusting the load rather than replacing the template.

The most problematic issue faced by conventional molding molds is the preparation of nano-features. Excitingly, the proposed CMG mold can facilitate the solution of this problem. To validate this, AAO templates with a pore size of about 300 nm were used to prepare CMG molds with nano features. Fig. 4(a) shows the SEM morphology of the AAO template with nanopore arrays, the corresponding stereomorphs were determined by AFM and are shown in Fig. 4(b-c). By applying a pressure of 1 kN to MG in the SLR, the nano-features on the AAO template were successfully replicated. Subsequently, the MG was converted to CMG by annealing. As shown in Fig. 4(d), CMG molds with nano-protrusion arrays were successfully prepared. The AFM images in Figs. 4(e-f) further illustrate the contours of the protrusions, we can find that they are homogeneous and no defects can be found. Eventually, the prepared nano-

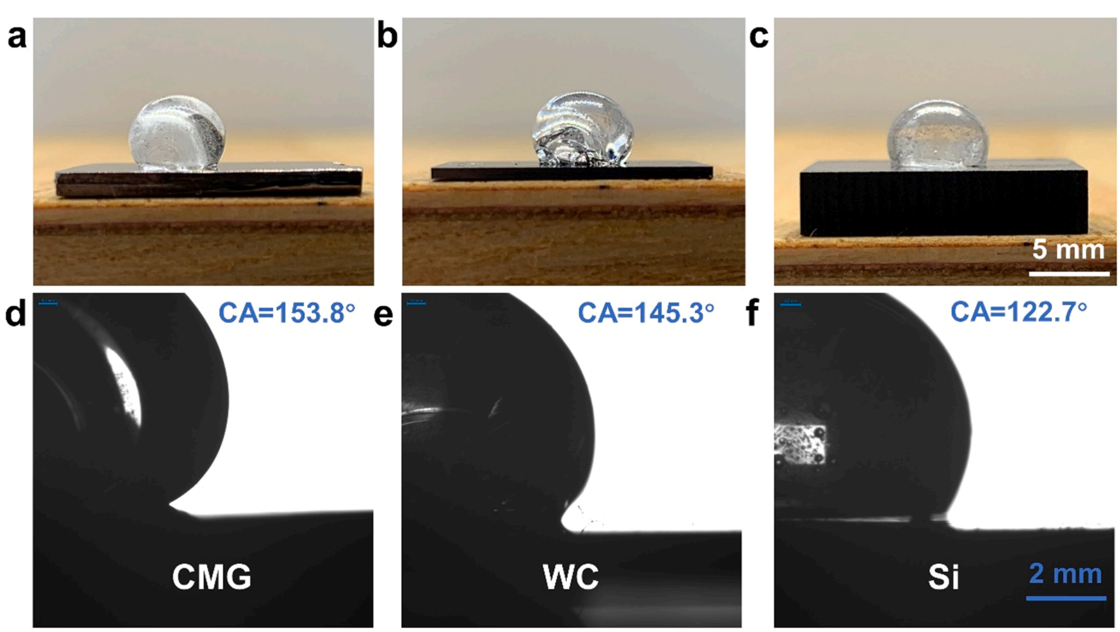

Fig. 2. (a-c) The contact states of molten glass on polished CMG, WC, and Si, respectively. (d-f) The corresponding CA value of the molten glass.

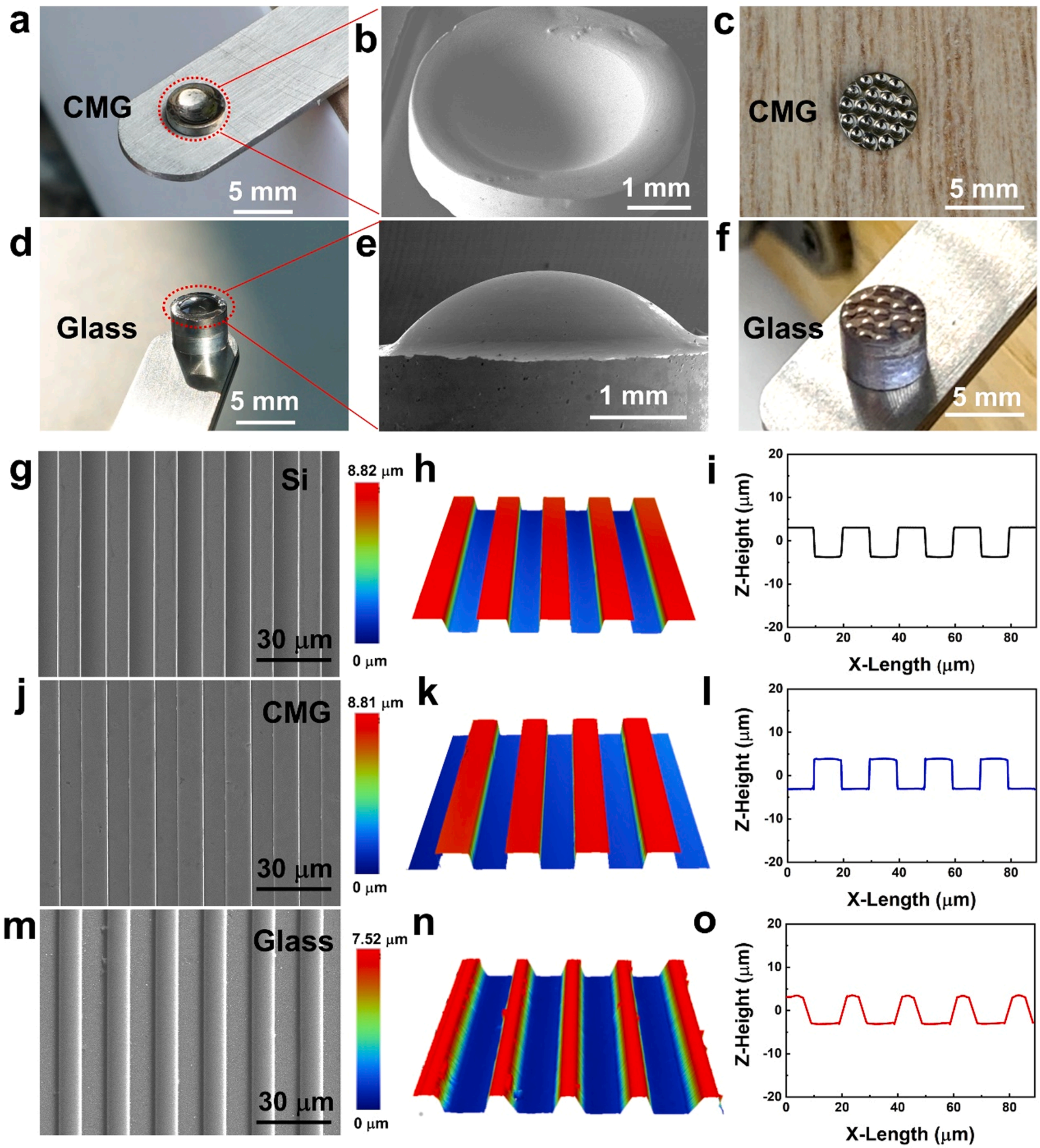

Fig. 3. (a) CMG mold of single lens. (b) SEM morphology corresponding to (a). (c) CMG mold lens array. (d) The glass component molded using the CMG mold in (a). (e) Side view of (d). (f) The glass component molded using the CMG mold in (c). (g-i) Morphology and dimensions of Si template (j-l) Morphology and dimensions of CMG molds prepared by Si template. (m-o) Morphology and dimensions of glass components prepared by CMG molds.

CMG mold was used to mold optical glasses to verify its usability. As displayed in the Fig. 4(g), lenticular arrays with nano-features were successfully prepared on optical glass. The AFM results in Fig. 4(h-i) demonstrate the concave profile of optical glasses, which is consistent with the profile of the AAO template. The successful preparation of nano-lens arrays on glass surfaces demonstrates the high applicability of the proposed CMG mold for nano-scale glass molding, which circumvents the fabrication challenges in conventional mold manufacturing process and opens a window for glass processing at the nano-scale.

The proposed CMG is a fast and low-cost method for the preparation of glass molding dies, which finds a convenient solution for the precision fabrication of hierarchical glass components. To validate the availability of this method, the properties of glass products prepared by CMG mold molding are examined. It is known that grating diffracts light at a certain angle according to the grating equation. When a compound light (such as sunlight) is shone on a grating, each beam of the compound light will separate in some direction, thus revealing a distinct grating pattern [45]. As shown in Fig. 5(a), the glass products (corresponding to Fig. 3(m-o)) molded from CMG molds exhibit color patterns visible to the eye, which indicates that the grating patterns on the Si template were successfully

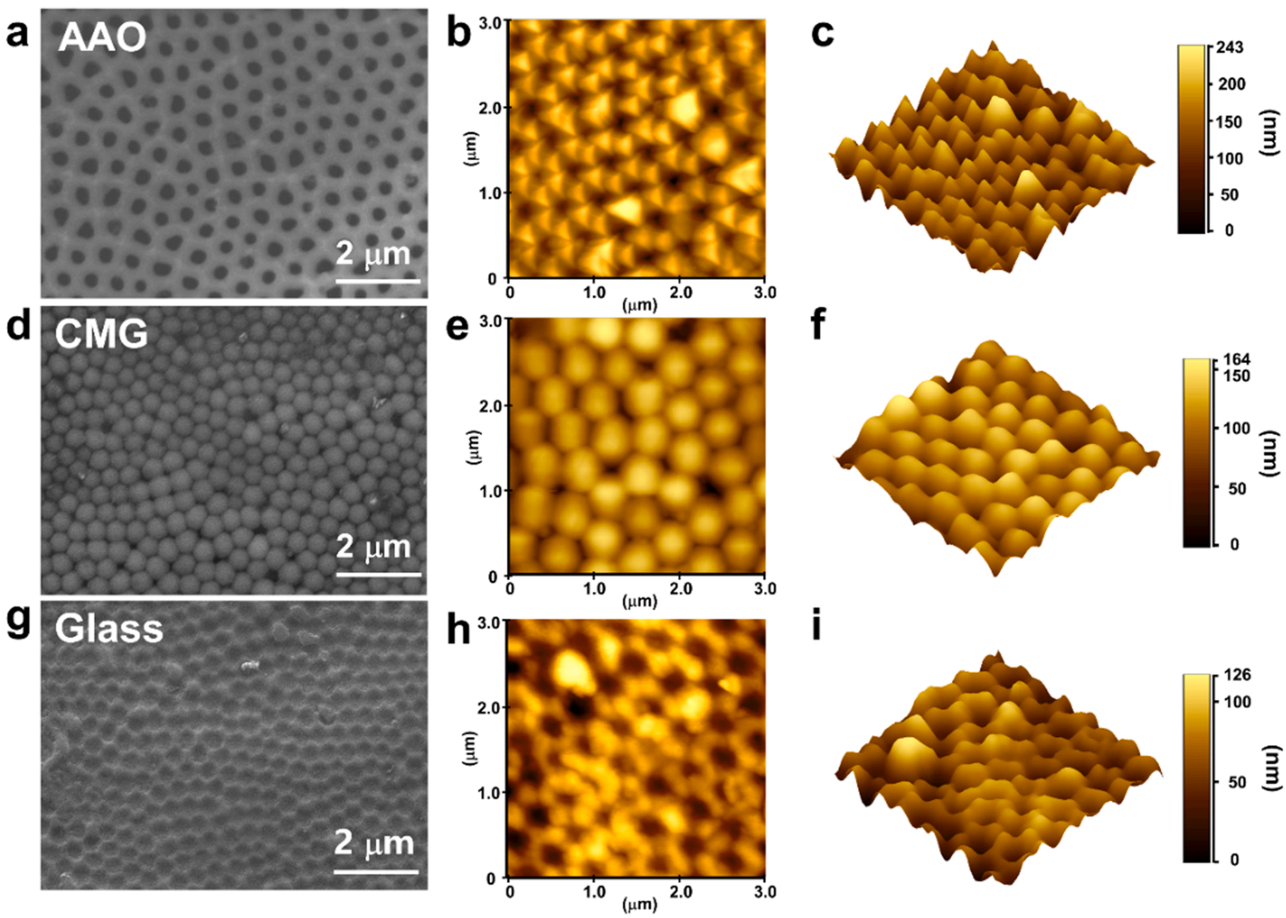

Fig. 4. (a-c) The SEM and AFM morphologys of AAO template. (d-f) The SEM and AFM morphologys of corresponding CMG molds. (g-i) The SEM and AFM morphologys of the optical glass surface obtained by CMG mold molding.

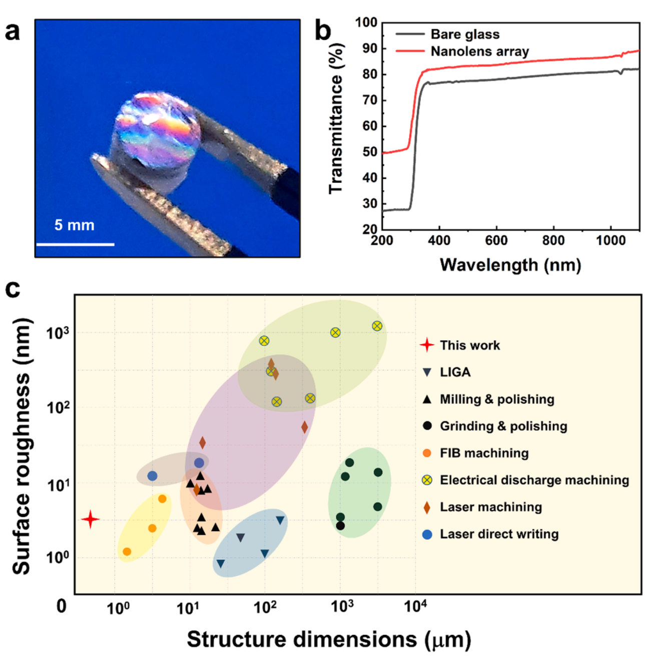

Fig. 5. (a) The photographic of grating glass product. (b) Comparison of light transmittance between nanostructured glass and bare glass. (c) A visualization map of optical mold preparation technologies.

transferred to the glass surface. In addition, glass with nanostructures shows better readability and light transmission than bare glass according to previous reports [5,46]. In this work, the light transmission of the glass products with nano-lens array (mentioned in Fig. 4 (g-i)) was measured. As shown in Fig. 5(b), glasses with nanoarrays show a significant increase in light transmission in the 200–1100 nm wavelength band compared to bare glass. One can see the improvement of about 23% in the 200–300 nm band and about 8% in the 300–1100 nm band, the results indicate that the use of the CMG mold to construct glass products with nano features is reliable.

As an emerging cutting-edge metallic material, MG brings the dawn of convenient precision manufacturing due to its unique superplasticity. In this work, CMG molds were developed for the molding of optical glass based on the superplasticity of MG. Compared to other mold preparation technologies, such as LIGA, ultra-precision milling/polishing/grinding, FIB machining, electrical discharge machining (EDM), laser machining, laser direct writing, CMG method provides significant convenience and cost-effectiveness. Surface roughness and minimum structure dimensions are two important considerations for mold preparation technology. The above two indicators of CMG method and other mentioned mold preparation technologies were summarized (See Table 1). To facilitate comparison, the visual mapping of surface roughness and minimum structural dimensions based on typical mold manufacturing technologies, including CMG method, was plotted. Different from other preparation techniques, the preparation of CMG molds is based on the thermoplastic forming of MG. Through thermoplastic molding, MG can achieve atomic-level surface roughness [47] and structures with a minimum feature size of 13 nm [28]. The optimal surface roughness of the CMG mold prepared in this work is 7.43 nm, and the smallest lens

Table 1
A summary of typical mold fabrication techniques.

Method	Surface roughness (nm)	Structure dimensions (μm)	Refs.
CMG	7.42	0.3	This work
LIGA	1.23	100	[48]
	6.61	300	[49]
	0.95	36–96	[50]
	4	62	[51]
Milling & polishing	<10	20	[52]
	3.2	11–39	[53]
	<10	15	[54]
	20	25	[55]
	<10	10	[56]
	2.3	<50	[57]
	3	20–30	[58]
	9	20–30	[59]
Grinding & polishing	18	5×10^3	[60]
	5.7	$<1 \times 10^3$	[61]
	<5	$<1 \times 10^3$	[62]
	30	1.5×10^3	[63]
	15.2	1.3×10^3	[64]
	7–23	5×10^3	[65]
FIB Machining	8	7	[66]
	1.4	2.5–4.93	[67]
	4.5	5	[68]
Electrical discharge machining	850	100	[69]
	196.6	700	[70]
	1×10^3	900	[71]
	219	300	[72]
	500	150	[73]
	2×10^3	5×10^3	[74]
Laser machining	700	200	[75]
	500	300	[76]
	9.5	20.5	[77]
	16.3	2	[78]
	80	500	[68]
Laser direct writing	27	25	[79]
	20	5	[80]

size is about 300 nm. As presented in Fig. 5(c), CMG method shows obvious advantages over other mold manufacturing technologies. This means that CMG method not only provides convenience, but also offers significant advantages in terms of manufacturing accuracy and minimum structural dimensions. To sum up, we developed a potential technique for the precise fabrication of nano-molds, which will advance the massive application of multifunctional nano-optical glass devices.

4. Conclusions

In summary, this work proposed a CMG method for the precision manufacturing of hierarchical optical molding molds. By using such method, multi-scale molds include macro lens arrays, micro grating and nano-lens arrays were successfully fabricated with reliable quality. The optimum surface roughness of the CMG mold prepared in this work was measured to be 7.43 nm, and the smallest lens size was about 300 nm. Utilizing the developed CMG molds, the corresponding optical glass components were prepared by PGM. The glass with grating exhibit color patterns visible to the eye and glass with nanoarrays show a significant increase of light transmission in the 200–1100 nm wavelength band compared to bare glass. The light transmission increased by 23% in the 200–300 nm band and by 8% in the 300–1100 nm band. To sum up, our results provide a fast and cost-efficient method for the mass production of optical molds and throw light on the precision fabrication of nanoscale optical devices.

CRediT authorship contribution statement

Fei Sun: Data curation, Writing – original draft, Investigation. **Jian Yang:** Data curation, Writing – original draft, Investigation. **Jianan Fu:** Investigation, Formal analysis. **Bei Wang:** Investigation, Formal analysis. **Jiang Ma:** Writing – review & editing. **Jun Shen:** Supervision.

Declaration of Competing Interest

The authors declare that they have no known competing financial interests or personal relationships that could have appeared to influence the work reported in this paper.

Data Availability

Data will be made available on request.

Acknowledgments

The work was supported by the Key Basic and Applied Research Program of Guangdong Province, China (Grant Nr. 2019B030302010), the NSF of China (Grant Nr.52122105, 51871157,51971150), the National Key Research and Development Program of China (Grant No. 2018YFA0703604). The authors also thank the assistance on microscope observation received from the Electron Microscope Center of the Shenzhen University.

References

[1] X. Liu, K. Li, J. Shen, F. Gong, Hot embossing of moth eye-like nanostructure array on transparent glass with enhanced antireflection for solar cells, Ceram. Int. 47 (2021) 18367–18375, https://doi.org/10.1016/j.ceramint.2021.03.159.
[2] Z. Ma, X. Hu, Y. Zhang, X. Liu, Z. Hou, L. Niu, L. Zhu, B. Han, Q. Chen, H. Sun, Smart compound eyes enable tunable imaging, Adv. Funct. Mater. 29 (2019) 1903340–1903350, https://doi.org/10.1002/adfm.201903340.
[3] Y. Lee, S.I. Bae, J. Eom, H.C. Suh, K.H. Jeong, Antireflective glass nanoholes on optical lenses, Opt. Express 26 (2018) 14786–14791, https://doi.org/10.1364/OE.26.014786.
[4] K. Jiang, K. Li, G. Xu, F. Gong, X. Wu, D. Diao, L. Zhu, A novel and flexible processing for hot embossing of glass microfluidic channels, Ceram. Int. 47 (2021) 1447–1455, https://doi.org/10.1016/j.ceramint.2020.09.253.
[5] Y. Feng, X. Liu, K. Li, F. Gong, J. Shen, Y. Lou, Glass flow evolution and the mechanism of antireflective nanoprotrusion arrays in nanoholes by direct thermal imprinting, ACS Appl. Mater. Interfaces 13 (2021) 16968–16977, https://doi.org/10.1021/acsami.0c22133.
[6] K. Li, G. Xu, X. Liu, F. Gong, Deformation behavior of glass nanostructures in hot embossing, ACS Appl. Mater. Interface 12 (2020) 36311–36319, https://doi.org/10.1021/acsami.0c08435.
[7] K. Li, X. Huang, Q. Chen, G. Xu, Z. Xie, Y. Wan, F. Gong, Flexible fabrication of optical glass micro-lens array by using contactless hot embossing process, J. Manuf. Process. 57 (2020) 469–476, https://doi.org/10.1016/j.jmapro.2020.07.019.
[8] J.J. Mecholsky Jr, S.W. Freiman, R.W. Rice, Effect of grinding on flaw geometry and fracture of glass, J. Am. Ceram. Soc. 60 (1977) 114–117, https://doi.org/10.1111/j.1151-2916.1977.tb15484.x.
[9] W. Gu, Z. Yao, H. Li, Investigation of grinding modes in horizontal surface grinding of optical glass BK7, J. Mater. Process. Technol. 211 (2011) 1629–1636, https://doi.org/10.1016/j.jmatprotec.2011.05.006.
[10] N. Belkhir, T. Aliouane, D. Bouzid, Correlation between contact surface and friction during the optical glass polishing, Appl. Surf. Sci. 288 (2014) 208–214, https://doi.org/10.1016/j.apsusc.2013.10.008.
[11] R.J. Wang, C.Y. Wang, W. Wen, J. Wang, Experimental study on a micro-abrasive slurry jet for glass polishing, Int. J. Adv. Manuf. Tech. 89 (2017) 451–462, https://doi.org/10.1007/s00170-016-9109-z.
[12] S. Bouzid, N. Bouaouadja, Effect of impact angle on glass surfaces eroded by sand blasting, J. Eur. Ceram. Soc. 20 (2000) 481–488, https://doi.org/10.1016/s0955-2219(99)00140-5.
[13] G. Kunkemöller, T.W. Maß, A.K.U. Michel, H.S. Kim, S. Brose, S. Danylyuk, T. Taubner, L. Juschkin, Extreme ultraviolet proximity lithography for fast, flexible and parallel fabrication of infrared antennas, Opt. Express 23 (2015) 25487–25495, https://doi.org/10.1364/oe.23.025487.
[14] K.K. Kwon, K.Y. Song, J.M. Seo, C.N. Chu, S.H. Ahn, Precise glass microstructuring with laser induced backside wet etching using error-compensating scan path, J. Mater. Process. Technol. 291 (2021), 117046, https://doi.org/10.1016/j.jmatprotec.2021.117046.
[15] Y. He, T. Zhou, X. Dong, P. Liu, W. Zhao, X. Wang, Y. Hu, J. Yan, Generation of high-saturation two-level iridescent structures by vibration-assisted fly cutting, Mater. Des. 193 (2020) 1–12, https://doi.org/10.1016/j.matdes.2020.108839.
[16] R.Q. Hsu, H.B. Wang, D.L. Liang, Hot embossing of parallel v-groove microstructures on glass, J. Am. Ceram. Soc. 92 (2009) 2605–2608, https://doi.org/10.1111/j.1551-2916.2009.03257.x.

[17] C.Y. Huang, C.C. Chen, H.Y. Chou, C.P. Chou, Fabrication of fresnel lens by glass molding technique, Opt. Rev. 20 (2013) 3, https://doi.org/10.1007/s10043-013-0035-0.
[18] W. Ming, Z. Chen, J. Du, Z. Zhang, G. Zhang, W. He, J. Ma, F. Shen, A comprehensive review of theory and technology of glass molding process, Int. J. Adv. Manuf. Technol. 107 (2020) 2671–2706, https://doi.org/10.1007/s00170-020-05051-0.
[19] Y. Saotome, K. Imai, N. Sawanobori, Microformability of optical glasses for precision molding, J. Mater. Process. Technol. 140 (2003) 379–384, https://doi.org/10.1016/s0924-0136(03)00828-8.
[20] X. Zhang, L. Li, Z. Li, C. Chan, L. Zhu, W. Lee, F. Fang, Highly uniform manufacturing method for large-area microlens arrays, Int. J. Adv. Manuf. Technol. 95 (2017) 99–108, https://doi.org/10.1007/s00170-017-1107-2.
[21] Y. Zhang, R. Liang, O.J. Spires, S. Yin, A. Yi, T.D. Milster, Precision glass molding of diffractive optical elements with high surface quality, Opt. Lett. 45 (2020) 6438–6441, https://doi.org/10.1364/OL.406195.
[22] M.A. Asgar, J. Kim, M.R. Haq, T. Kim, S.M. Kim, A comprehensive review of micro/nano precision glass molding molds and their fabrication methods, Micromachines (Basel) (2021) 12, https://doi.org/10.3390/mi12070812.
[23] F. Sun, B. Wang, F. Luo, Y.Q. Yan, H.B. Ke, J. Ma, J. Shen, W.H. Wang, Shear punching of bulk metallic glasses under low stress, Mater. Des. 190 (2020), 108595, https://doi.org/10.1016/j.matdes.2020.108595.
[24] F. Luo, F. Sun, K. Li, F. Gong, X. Liang, X. Wu, J. Ma, Ultrasonic assisted micro-shear punching of amorphous alloy, Mater. Res. Lett. 6 (2018) 545–551, https://doi.org/10.1080/21663831.2018.1500399.
[25] J. Ma, C. Yang, X. Liu, B. Shang, Y. Yang, Fast surface dynamics enabled cold joining of metallic glasses, Sci. Adv. 5 (2019) eaax7256, https://doi.org/10.1126/sciadv.aax7256.
[26] G. Duan, A. Wiest, M.L. Lind, J. Li, W.K. Rhim, W.L. Johnson, Bulk metallic glass with benchmark thermoplastic processability, Adv. Mater. (2007) 4272–4275, https://doi.org/10.1002/adma.200700969.
[27] J. Schroers, Q. Pham, A. Peker, N. Paton, R.V. Curtis, Blow molding of bulk metallic glass, Scr. Mater. 57 (2007) 341–344, https://doi.org/10.1016/j.scriptamat.2007.04.033.
[28] G. Kumar, H.X. Tang, J. Schroers, Nanomoulding with amorphous metals, Nature 457 (2009) 868–872, https://doi.org/10.1038/nature07718.
[29] Y.H. Liu, G. Wang, R.J. Wang, D.Q. Zhao, M.X. Pan, W.H. Wang, Super plastic bulk metallic glasses at room temperature, Science 315 (2007) 1385–1388, https://doi.org/10.1126/science.1136726.
[30] J. Schroers, The superplastic forming of bulk metallic glasses, JOM 57 (2005) 35–39, https://doi.org/10.1007/s11837-005-0093-2.
[31] P. He, L. Li, F. Wang, O. Dambon, F. Klocke, K. M, F. Allen, Y. Yi, Bulk metallic glass mold for high volume fabrication of micro optics, Microsyst. Technol. 22 (2016) 617–623, https://doi.org/10.1007/s00542-014-2395-1.
[32] N. Zhang, J.S. Chu, C.J. Byrne, D.J. Browne, M.D. Gilchrist, Replication of micro/nano-scale features by micro injection molding with a bulk metallic glass mold insert, J. Micromech. Microeng. (2012) 22, https://doi.org/10.1088/0960-1317/22/6/065019.
[33] J.P. Singer, M. Gopinadhan, Z. Shao, A.D. Taylor, J. Schroers, C.O. Osuji, Nanoimprinting sub-100nm features in a photovoltaic nanocomposite using durable bulk metallic glass molds, ACS Appl. Mater. Interfaces 7 (2015) 3456–3461, https://doi.org/10.1021/am507368g.
[34] J. Ma, X. Zhang, W.H. Wang, Metallic glass mold insert for hot embossing of polymers, J. Appl. Phys. (2012) 112, https://doi.org/10.1063/1.4737484.
[35] X. Liu, Y. Shao, S.Y. Lu, K.F. Yao, High-accuracy bulk metallic glass mold insert for hot embossing of complex polymer optical devices, J. Polym. Sci. Part B Polym. Phys. 53 (2015) 463–467, https://doi.org/10.1002/polb.23670.
[36] J.J. He, N. Li, N. Tang, X.Y. Wang, C. Zhang, L. Liu, The precision replication of a microchannel mould by hot-embossing a Zr-based bulk metallic glass, Intermetallics 21 (2012) 50–55, https://doi.org/10.1016/j.intermet.2011.10.001.
[37] A. Inoue, T. Zhang, Fabrication of bulk glassy Zr55Al10Ni5Cu30 alloy of 30 mm in diameter by a suction casting method, Mater. Trans. JIM 37 (1996) 185–187, https://doi.org/10.2320/matertrans1989.37.185.
[38] A.N. Akdogan, M.N. Durakbasa, Thermal cycling experiments for glass moulds surface texture lifetime prediction – Evaluation with the help of statistical techniques, Measurement 41 (2008) 697–703, https://doi.org/10.1016/j.measurement.2007.10.006.
[39] D. Zhonga, E. Mateevaa, I. Dahanb, J.J. Moorea, G.G.W. Mustoea, T. Ohnoa, J. Disamc, S. Thielc, Wettability of Ni-Al, Ni-Al-N, Ti-B-C, and Ti-B-C-N films by glass at high temperatures, Surf. Coat. Technol. (2000), https://doi.org/10.1016/S0257-8972(00)00877-X.
[40] X.Y. Zhu, J.J. Wei, L.X. Chen, J.L. Liu, L.F. Hei, C.M. Li, Y. Zhang, Anti-sticking *Re*-Ir coating for glass molding process, Thin Solid Films 584 (2015) 305–309, https://doi.org/10.1016/j.tsf.2015.01.002.
[41] Y.Y. Chang, C.M. Cheng, Y.Y. Liou, W. Tillmann, F. Hoffmann, T. Sprute, High temperature wettability of multicomponent CrAlSiN and TiAlSiN coatings by molten glass, Surf. Coat. Technol. 231 (2013) 24–28, https://doi.org/10.1016/j.surfcoat.2012.04.050.
[42] Fundamentals of glass-to-metal bonding: VIII, nature of wetting and adherence, J. Am. Ceram. Soc. (1962) 45, https://doi.org/10.1111/j.1151-2916.1962.tb11067.x.
[43] Y. Zhang, G. Yan, K. You, F. Fang, Study on α-Al_2O_3 anti-adhesion coating for molds in precision glass molding, Surf. Coat. Technol. (2020) 391, https://doi.org/10.1016/j.surfcoat.2020.125720.
[44] C.L. Chao, C.B. Huo, W.C. Chou, Y.R. Lin, K.J. Ma, H.H. Chien, Study on the design of precious metal based protective films for glass moulding process, Surf. Coat. Technol. 231 (2013) 567–572, https://doi.org/10.1016/j.surfcoat.2012.10.066.
[45] J. Ma, J. Yi, D.Q. Zhao, M.X. Pan, W.H. Wang, Large size metallic glass gratings by embossing, J. Appl. Phys. 112 (2012), 064505, https://doi.org/10.1063/1.4752399.
[46] H. Jung, K.H. Jeong, Monolithic polymer microlens arrays with antireflective nanostructures, Appl. Phys. Lett. (2012) 101, https://doi.org/10.1063/1.4747717.
[47] G. Kumar, P.A. Staffier, J. Blawzdziewicz, U.D. Schwarz, J. Schroers, Atomically smooth surfaces through thermoplastic forming of metallic glass, Appl. Phys. Lett. (2010) 97, https://doi.org/10.1063/1.3485298.
[48] T.H. Lin, S.Y. Hung, H. Yang, C.K. Chao, Fabrication of a microlens array electroformed mold with low roughness and high hardness, J. Micromech. Microeng. 17 (2007) 419–425, https://doi.org/10.1088/0960-1317/17/3/001.
[49] D.S. Kim, H.S. Lee, B.-.K. Lee, S.S. Yang, T.H. Kwon, S.S. Lee, Replications and analysis of microlens array fabricated by a modified LIGA process, Polym. Eng. Sci. 46 (2006) 416–425, https://doi.org/10.1002/pen.20466.
[50] S.-d. moon, N. Lee, S. Kang, Fabrication of a microlens array using micro-compression molding with an electroformed mold insert, J. Micromech. Microeng. 13 (2003) 98–103, https://doi.org/10.1088/0960-1317/13/1/314.
[51] K.H. Liu, M.F. Chen, C.T. Pan, M.Y. Chang, W.Y. Huang, Fabrication of various dimensions of high fill-factor micro-lens arrays for OLED package, Sens. Actuators A 159 (2010) 126–134, https://doi.org/10.1016/j.sna.2010.02.020.
[52] Fritz Klocke, Olaf Dambon, Benjamin Bulla, M. Heselhaus, Direct diamond turning of steel molds for optical replication, in: 4th International Symposium on Advanced Optical Manufacturing and Testing Technologies: Advanced Optical Manufacturing Technologies, Germany, 2009, pp. 1–7.
[53] Y. Takeuchi, S. Maeda, T. Kawai, K. Sawada, Manufacture of multiple-focus micro Fresnel lenses by means of nonrotational diamond grooving, CIRP Ann. 51 (2002) 343–346, https://doi.org/10.1016/s0007-8506(07)61532-7.
[54] J. Osmer, R. Gläbe, O. Riemer, E. Brinksmeier, S. Bütepage, F. Hoffmann, Diamond milling of nitrided steels for optical mold making, J. Vac. Sci. Technol. B Microelectron. Nanom. Struct. Process. Meas. Phenom. 27 (2009), https://doi.org/10.1116/1.3049512.
[55] M.L. Hupert, W.J. Guy, S.D. Llopis, H. Shadpour, S. Rani, D.E. Nikitopoulos, S. A. Soper, Evaluation of micromilled metal mold masters for the replication of microchip electrophoresis devices, Microfluid. Nanofluid. 3 (2006) 1–11, https://doi.org/10.1007/s10404-006-0091-x.
[56] A.K. Holthusen, O. Riemer, J. Schmütz, A. Meier, Mold machining and injection molding of diffractive microstructures, J. Manuf. Process 26 (2017) 290–294, https://doi.org/10.1016/j.jmapro.2017.02.014.
[57] R. Gläbe, O. Riemer, Diamond machining of micro-optical components and structures, in: micro-Optics 2010, SPIE (2010) 15–24.
[58] E. Brinksmeier, R. Gläbe, Diamond machining of steel molds for optical applications, Key Eng. Mater. 364-366 (2007) 701–706, https://doi.org/10.4028/www.scientific.net/KEM.364-366.701.
[59] L. Li, A.Y. Yi, C. Huang, D.A. Grewell, A. Benatar, Y. Chen, Fabrication of diffractive optics by use of slow tool servo diamond turning process, Opt. Eng. 45 (2006), 113401, https://doi.org/10.1117/1.2387142.
[60] H. Suzuki, T. Furuki, M. Okada, Y. Yamagata, S. Morita, Precision grinding of structured tungsten carbide mold, Adv. Mater. Res. 497 (2012) 15–19, https://doi.org/10.4028/www.scientific.net/AMR.497.15.
[61] M.A. Maher, Y.E. Tohme, H.D. Stewart, J.C. Chiao, T.J. Suleski, E.G. Johnson, G. P. Nordin, Grinding aspheric and freeform micro-optical molds, in: micromachining technology for micro-optics and nano-optics V and microfabrication process technology XII, Winchester, 2007, pp. 1–8.
[62] E.G. Johnson, H. Owari, G.P. Nordin, S. Kawai, Y. Mukai, T.J. Suleski, S. Terada, T. Matsuo, M. Seigo, A. Yano, T. Imura, D. Emi, S. Kitagawa, Technology development of mold fabrication for free-form surface DOE, and microlens,, Micromachining Technology for Micro-optics and Nano-optics IV (2006) 1–10.
[63] E. Brinksmeier, O. Riemer, A. Gessenharter, L. Autschbach, Polishing of structured molds, CIRP Ann. 53 (2004) 247–250, https://doi.org/10.1016/s0007-8506(07)60690-8.
[64] T. Bletek, F. Klocke, M. Hünten, O. Dambon, Dressing of grinding wheels for ultra precision grinding of diffractive structures in tungsten carbide molds, Key Eng. Mater. 625 (2014) 161–166, https://doi.org/10.4028/www.scientific.net/KEM.625.161.
[65] Kinematics in ultra-precision grinding of WC moulds, Int. J. Nanomanuf. 7 (2011) 199–213, https://doi.org/10.1504/ijnm.2011.042464.
[66] Y. Fu, Investigation of microlens mold fabricated by focused ion beam technology, Microelectron. Eng. 56 (2001) 333–338, https://doi.org/10.1016/s0167-9317(01)00570-6.
[67] K. Watanabe, T. Morita, R. Kometani, T. Hoshino, K. Kondo, K. Kanda, Y. Haruyama, T. Kaito, J. Fujita, M. Ishida, T. Tajima, S. Matsui, Y. Ochiai, Nanoimprint using three-dimensional microlens mold made by focused-ion-beam chemical vapor deposition, J. Vac. Sci. Technol. B 22 (2004) 22–26, https://doi.org/10.1116/1.1633281.
[68] S.W. Youn, M. Takahashi, H. Goto, R. Maeda, Fabrication of micro-mold for glass embossing using focused ion beam, femto-second laser, eximer laser and dicing techniques, J. Mater. Process. Technol. 187-188 (2007) 326–330, https://doi.org/10.1016/j.jmatprotec.2006.11.120.
[69] H. Takino, T. Hosaka, Shaping of steel mold surface of lens array by electrical discharge machining with spherical ball electrode, Appl. Opt. 55 (2016) 4967–4973, https://doi.org/10.1364/AO.55.004967.

[70] H. Huang, J. Yan, On the surface characteristics of a Zr-based bulk metallic glass processed by microelectrical discharge machining, Appl. Surf. Sci. 355 (2015) 1305–1315, https://doi.org/10.1016/j.apsusc.2015.08.239.

[71] H. Takino, T. Hosaka, Shaping of steel mold surface of lens array by electrical discharge machining with single rod electrode, Appl. Opt. 53 (2014) 8002–8005, https://doi.org/10.1364/AO.53.008002.

[72] M. Sorgato, D. Masato, G. Lucchetta, Effects of machined cavity texture on ejection force in micro injection molding, Precis. Eng. 50 (2017) 440–448, https://doi.org/10.1016/j.precisioneng.2017.06.019.

[73] Z. Huang, X. Liang, C. Chang, J. Ma, WEDM-LS processing sophisticated and durable Zr-based metallic glass mold insert for micro structure injection of polymers, Biomed. Microdevices 21 (2019) 13, https://doi.org/10.1007/s10544-019-0366-0.

[74] T. Zhou, F. Ma, B. Ruan, J. Zhou, P. Liew, X. Wang, Microlens array fabrication on WC mold using EDM milling with *in situ* electrode trimming, Int. J. Adv. Manuf. Technol. 103 (2019) 3003–3011, https://doi.org/10.1007/s00170-019-03731-0.

[75] C.Y. Huang, C.H. Kuo, W.T. Hsiao, K.C. Huang, S.F. Tseng, C.P. Chou, Glass biochip fabrication by laser micromachining and glass-molding process, J. Mater. Process. Technol. 212 (2012) 633–639, https://doi.org/10.1016/j.jmatprotec.2011.10.013.

[76] A. Selada, A. Manaia, M.T. Vieira, A.S. Pouzada, Effect of LBM and large-area EBM finishingon micro-injection moulding surfaces, Int. J. Adv. Manuf. Technol. 52 (2011) 171–182, https://doi.org/10.1007/s00170-010-2723-2.

[77] C. Kim, I.B. Sohn, Y.J. Lee, C.C. Byeon, S.Y. Kim, H. Park, H. Lee, Fabrication of a fused silica based mold for the microlenticular lens array using a femtosecond laser and a CO2 laser, Opt. Mater. Express 4 (2014) 2233–2240, https://doi.org/10.1364/OME.4.002233.

[78] Z. Gan, X. Peng, C. Guan, Machining of optical micro-mold by laserinduced chemical etching, AIP Adv. 9 (2019), 005106, https://doi.org/10.1063/1.5095590.

[79] M. Roeder, D. Hera, S. Thiele, W. Osten, 3D Laser Direct-Writing Based Mold Fabrication For the Manufacturing of Diffractive-Refractive Elements, Hahn Schickard, Germany, 2017, pp. 1–21.

[80] M. Roedera, S. Thieleb, D. Heraa, C. Prussb, T. Guenthera, W. Ostenb, A. Zimmermann, Fabrication of curved diffractive optical elements by means of laser direct writing, electroplating, and injection compression molding, J. Manuf. Process 47 (2019) 402–409, https://doi.org/10.1016/j.jmapro.2019.10.012.